

Torsional magnetic reconnection at three dimensional null points: A phenomenological study

Peter Wyper and Rekha Jain

Citation: *Physics of Plasmas* **17**, 092902 (2010); doi: 10.1063/1.3480639

View online: <http://dx.doi.org/10.1063/1.3480639>

View Table of Contents: <http://aip.scitation.org/toc/php/17/9>

Published by the *American Institute of Physics*



Small Conferences. BIG Ideas.

Applied Physics
Reviews

SAVE THE DATE!
3D Bioprinting: Physical and Chemical Processes
May 2–3, 2017 • Winston Salem, NC, USA

The background of the banner features a stylized, glowing blue and red structure resembling a biological or physical network, possibly representing a 3D bioprinted structure or a complex physical process.

Torsional magnetic reconnection at three dimensional null points: A phenomenological study

Peter Wyper and Rekha Jain

School of Mathematics and Statistics, University of Sheffield, Sheffield S3 7RH, United Kingdom

(Received 12 May 2010; accepted 6 July 2010; published online 21 September 2010)

Magnetic reconnection around three dimensional (3D) magnetic null points is the natural progression from X-point reconnection in two dimensions. In 3D the separator field lines of the X-point are replaced with the spine line and fan plane (the field lines which asymptotically approach or recede from the null). In this work analytical models are developed for the newly classified *torsional spine* and *torsional fan* reconnection regimes by solving the steady state, kinematic, resistive magnetohydrodynamic equations. Reconnection is localized to around the null through the use of a localized field perturbation leading to a localized current while a constant resistivity is assumed. For the torsional spine case current is found to localize around the spine leading to a spiraling slippage of the field around the spine and out along the fan. For the torsional fan case current is found to be localized to the fan plane leading again to a spiraling slippage of the field. In each case no flux is transported across either the spine or the fan. An intermediate twist is then introduced and a link is established between the two regimes. We find that for a general twist plasma flows associated with both torsional spine and fan appear in distinct regions. As such we suggest that the “pure” flows of each are extreme cases. © 2010 American Institute of Physics.

[doi:10.1063/1.3480639]

I. INTRODUCTION

Magnetic reconnection is a fundamental physical process of an astrophysical plasma. It is the restructuring of the magnetic field through the changing of the connectivity of the magnetic field lines. The majority of astrophysical plasmas including the solar corona, however, have low plasma resistivity so reconnection may only occur in regions where very intense currents develop. Therefore the key questions regarding reconnection in astrophysical plasmas are where do these intense currents develop and what effects do they have on the plasma flows and energy release?

This however is not an easy problem since the astrophysical plasmas have a very complex three dimensional (3D) magnetic structure. Recent efforts to understand magnetic reconnection in the solar corona have led to some progress. Two main scenarios have emerged during the investigation of the current sheet formation process: reconnection at and around 3D magnetic null points and their associated separator field lines—the field line that connects two nulls (for example, see Refs. 1–9). We focus here on reconnection around an isolated 3D null. The field topology in the vicinity of such a null is defined by two structures. The *fan* (or Σ -) plane, a continuum of field lines that asymptotically recede from (or approach) the null, and the *spine* (or γ -) line, two field lines that asymptotically approach (or recede from) the null. These structures may be found by examining the linearized field topology around the null defined by the equation

$$\mathbf{B} = \mathcal{M} \cdot \mathbf{r}, \quad (1)$$

where the matrix \mathcal{M} is given by the Jacobian of \mathbf{B} and \mathbf{r} the position vector $(x, y, z)^T$. The eigenvectors of \mathcal{M} (whose cor-

responding eigenvalues sum to zero since $\nabla \cdot \mathbf{B} = 0$) define the spine and fan such that the two eigenvalues whose real parts have like sign lie in the fan plane with the third directed along the spine line. The fan surface is a separatrix surface between two topologically unique regions. The spine cannot separate different regions being only a line but is still an important feature as changes in the symmetry within the regions separated by the fan manifest in a change in the field at or around the spine.

The existence of 3D nulls is predicted in abundance in the solar corona (e.g., Refs. 10–12). Proposed applications for null reconnection include sites for coronal heating¹³ and involvement in jets,^{14,15} solar flares,^{16,17} and coronal mass ejections.^{18,19} The evidence for 3D null point reconnection is also suggested in the Earth’s magnetotail on the basis of observations from the cluster satellites.²⁰

Although it is now accepted that reconnection at 3D null points is of great importance in realistic 3D field geometries, a full understanding of the different kinds of reconnection that occurs at these null points is still to be achieved. Early work using ideal steady state kinematic models^{3,9} suggested reconnection types that transported flux across the fan or spine. Later work by^{21,22} extended this to include a local diffusion region and constant current \mathbf{J} . Two different current cases were considered. When \mathbf{J} was parallel to the fan plane flux was found to cross both the spine and fan in a similar way as was suggested by Ref. 9. When \mathbf{J} was parallel to the spine however a rotational slippage of the field was found where no flux was transported across either the spine or fan but rotated around the spine symmetrically. Numerical experiments by Refs. 23 and 24 also found this rotational slippage but with currents diffused in one direction when the magnetic field is rotationally perturbed. Pontin and

Galsgaard²³ also noted that perturbing the fan or spine produced local currents focusing on the null with plasma flow across the fan or spine, respectively. The culmination of all these results led Pontin and Priest²⁵ to reclassify reconnection around 3D nulls into three types: *torsional fan* and *torsional spine* which involve spatially diffused currents in one direction leading to rotational slippage and *spine-fan* which covers all cases of flux transport across the spine or fan in the more traditional manner.

As noted, so far, all the steady state, kinematic models have been studied by localizing η . However, from simulation studies (for example, Refs. 23 and 24), localized currents have been seen with slippage of flux velocities around the spine and fan, and for applications to astrophysical plasma, it may also be interesting to explore the effect of localized current. This work aims to present steady kinematic models for torsional spine and torsional fan through the use of a localized current.

II. GENERAL METHOD

We seek to find solutions to the kinematic, steady state, resistive MHD equations in the vicinity of a 3D magnetic null point. Thus, we solve

$$\mathbf{E} + \mathbf{v} \times \mathbf{B} = \eta \mathbf{J}, \quad (2)$$

$$\nabla \times \mathbf{E} = 0, \quad (3)$$

$$\nabla \times \mathbf{B} = \mu_0 \mathbf{J}, \quad (4)$$

$$\nabla \cdot \mathbf{B} = 0. \quad (5)$$

From Eq. (3) we can express the electric field as $\mathbf{E} = -\nabla\Phi$ where Φ is a scalar potential. The component of Eq. (2) parallel to \mathbf{B} can be combined with this and integrated along the magnetic field lines to give

$$\Phi = - \int \eta \mathbf{J} \cdot \mathbf{B} ds + \Phi_0. \quad (6)$$

This integral is solved by using the field line equations in (r, ϕ, z) expressed in terms of the parameter s and some initial position (r_0, ϕ_0, z_0) . The field line equations are obtained by solving

$$\frac{dr}{B_r} = \frac{rd\phi}{B_\phi} = \frac{dz}{B_z} = ds. \quad (7)$$

These equations are invertible so Φ can be represented as a function of s and initial position to carry out the integral in Eq. (6) and then transferred back into a function of $r, \phi,$ and z to find the electric field from

$$\mathbf{E} = -\nabla\Phi. \quad (8)$$

Thus for a given magnetic configuration we can find the electric field due to nonideal effects (i.e., those due to $\mathbf{J} \neq \mathbf{0}$). Using this we can also find the resulting flow velocity perpendicular to the magnetic field by taking the vector product of Eq. (2) with \mathbf{B} to give

$$\mathbf{v}_\perp = \frac{(\mathbf{E} - \eta \mathbf{J}) \times \mathbf{B}}{B^2}. \quad (9)$$

In the next section, we consider a general perturbation in the ϕ -component of a simple linear magnetic field and investigate the properties of torsional reconnections using this general method.

III. TORSIONAL RECONNECTION

Consider

$$\mathbf{B} = B_0 [r, jr^\alpha z^\gamma (zr^2)^\beta e^{-(1/l^2)[a^2 r^2 + b^2 z^2 + c^2 (zr^2)^2]}, -2z], \quad (10)$$

where $\alpha, \beta,$ and γ are all either zero or positive integers and $a, b, c, l,$ and j are constants. This type of perturbation leads to a twist of the field lines around the spine and depending on the choice of parameters a rotational slippage of these field lines. In the following subsections, we investigate in detail the two main types of torsional reconnections.

A. Torsional spine

Consider the case $\gamma=0$ and $a=1; b=0$ in the above Eq. (10). Thus the field is of the form

$$\mathbf{B} = B_0 [r, jr^\alpha (zr^2)^\beta e^{-(1/l^2)[r^2 + c^2 (zr^2)^2]}, -2z]. \quad (11)$$

The field line equations for r and z can be found to be

$$r = r_0 e^{B_0 s}, \quad z = z_0 e^{-2B_0 s}. \quad (12)$$

Using these we can express the ϕ field line as

$$\phi = jB_0 (z_0 r_0^2)^\beta e^{-(c^2/l^2)(z_0 r_0^2)^2} F(\alpha - 1) + C, \quad (13)$$

where C is a constant of integration and $F(A)$ is defined as

$$F(A) = r_0^A \int e^{AB_0 s} e^{-(r_0^2/l^2)e^{2B_0 s}} ds. \quad (14)$$

Using integration by parts, it is easy to show a recurrence relation for F defined by

$$F(A + 2) = \frac{l^2}{2} \left(AF(A) - \frac{r^A}{B_0} e^{-r^2/l^2} \right), \quad (15)$$

and since

$$F(1) = \frac{l\sqrt{\pi}}{2B_0} \mathbf{erf}\left(\frac{r}{l}\right),$$

$$F(2) = -\frac{l^2 e^{-r^2/l^2}}{2B_0},$$

and the fact that $\alpha \geq 0$, we can find solutions for nonsingular fields. Here $\mathbf{erf}(\mathbf{x})$ is an error function. Using Eq. (4) we find

$$\mathbf{J} = \frac{jB_0}{\mu_0} \left(z^{-1} \left[-\beta + \frac{2c^2}{l^2} (zr^2)^2 \right], 0, r^{-1} \left\{ (2\beta + \alpha + 1) - \frac{2}{l^2} [r^2 + 2c^2 (zr^2)^2] \right\} \right) r^\alpha (zr^2)^\beta e^{-(1/l^2)[r^2 + c^2 (zr^2)^2]}, \quad (16)$$

and using Eq. (6) we find the electric potential

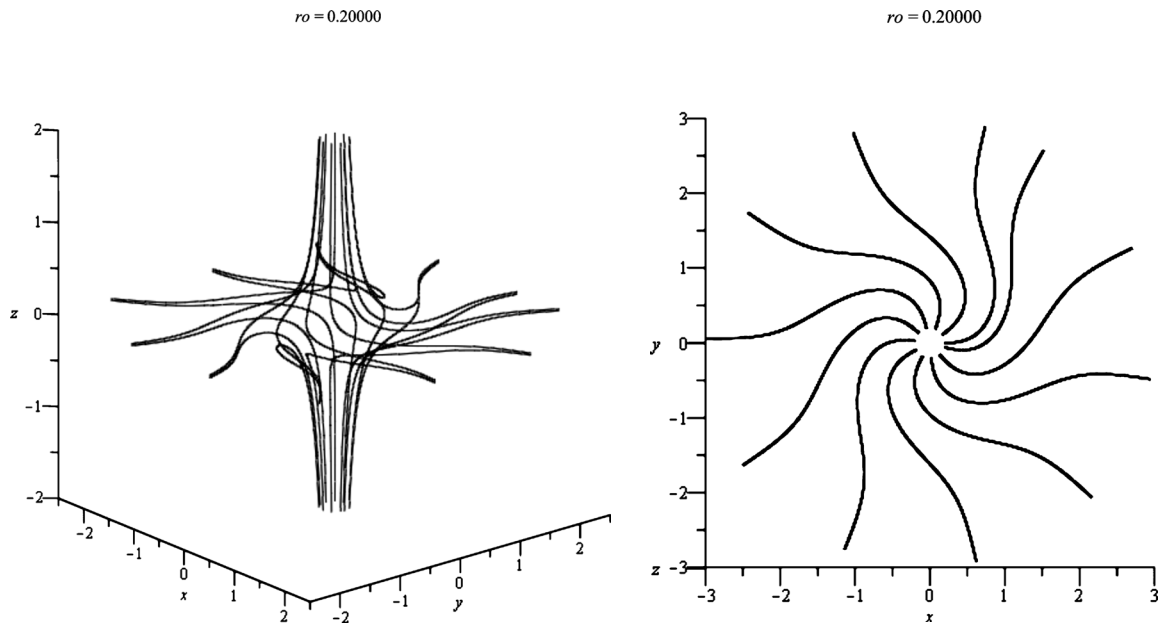


FIG. 1. Top and side views of field lines plotted for $\alpha=4$ and $\beta=0$ with $j=3$. The field lines close to the spine are approaching the null and receding away from the null in the fan plane.

$$\begin{aligned} \Phi = \frac{j\eta_0 B_0}{\mu_0} & \left[\left(\beta - \frac{2c^2}{l^2} (zr^2)^2 \right) F(\alpha+3) (zr^2)^{\beta-1} \right. \\ & - \frac{4}{l^2} F(\alpha-1) (zr^2)^{\beta+1} + 2 \left((\alpha+2\beta+1) \right. \\ & \left. \left. - \frac{4c^2}{l^2} (zr^2)^2 \right) F(\alpha-3) (zr^2)^{\beta+1} \right] e^{-(c^2/l^2)(zr^2)}, \quad (17) \end{aligned}$$

where $\alpha \neq 1$ or 3.

It is clear that depending on the choice of parameters the field will be perturbed differently. In the following subsections we investigate in more detail the reconnection process that occurs for these different types of perturbation.

Throughout the paper unless otherwise stated we shall consider $l = \eta_0 = \mu_0 = B_0 = 1$ with the plots being produced using MAPLE 13 with a relative scaling of (strength/maximum)^{1/d} (where $d=3$ unless otherwise stated) for clarity.

1. Same direction twist

For the field lines to be symmetric above and below the fan plane we must choose β to be *even* in conjunction with $\alpha > 0$, when $\alpha=0$ all values of β give rise to sinks and sources, such flows are unphysical.

a. The z independent case: $\beta=0$ and $c=0$.

Note from Eq. (17) that for $\beta=0$, the z -component of the electric field ($E_z = -\partial\Phi/\partial z$) is zero when $F(\alpha-3)/F(\alpha-1) = 2/(\alpha+1)l^2$ for $r \neq 0$. The total plasma flows, therefore, have sinks and sources in the rz -plane for all odd α values. Such flows are unphysical. From Eq. (16) it is clear that for $\beta=0$ a singular current results from $\alpha=0$. Also, $\alpha=2$ gives a nonzero $v_{\perp\phi}$ when $r=0$, which is not a realistic physical solution. Thus, for $\beta=0$, only even values of $\alpha \geq 4$ are permissible.

b. Even α .

Using $\alpha=4$ we get a field of the form

$$\mathbf{B} = B_0(r, jr^4 e^{-r^2/l^2}, -2z). \quad (18)$$

Figure 1 shows the resulting twisted field lines associated with this choice of parameters. We see a radially symmetric twist in the field that is localized to a toroidal region around the spine but which is unbounded in height. The value of l varies the strength of the damping from the exponential term which will stretch the toroidal region inward or outward. Outside the region we see the field lines straighten out as the field becomes more potential in nature. The current flows are found to be localized to the region of twist and exist in annular bands around the spine. Figure 2, left panel, shows them as opposite bands in the rz -plane. Such bands were also observed at intermediate time steps in the numerical simulations by Ref. 23. Recall that in our model, there is no current at the null itself so the field and the flows are more representative of the later stages of evolution after an initial disturbance.

Lastly, in the right and bottom panels of Fig. 2, we show the plasma velocity resulting from the twisting of the field lines. It appears that the plasma spirals down around the spine and then spirals out along the fan plane. As expected, the strongest flows occur within the region of greatest twist. For higher even values of α , the twist in the field is reduced (increased) where $r < l$ ($r > l$), with similar plasma and current flows. This kind of reconnection was also seen in the numerical simulation studies carried out by Ref. 23. They also find rotational plasma flows but their flows were affected by reflections of the pulse from the simulation box boundary creating counter rotating flows which we do not see here.

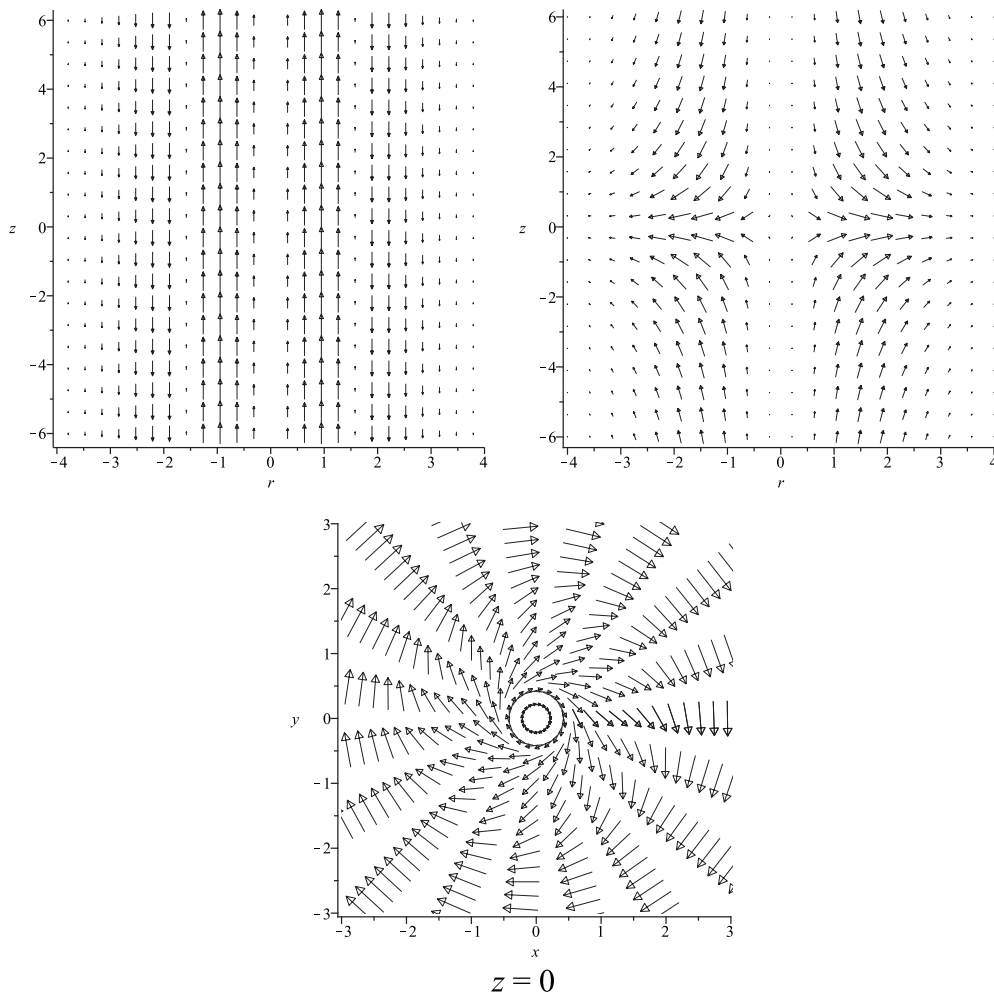


FIG. 2. The left panel shows a slice of the radially symmetric current flow. The right and bottom panels are the scaled plots of the plasma flow. These are plotted for $\alpha=4$ and $\beta=0$ with $j=3$. Note that here r denotes either x or y .

c. The z dependent case: $\beta \neq 0$ and $c \neq 0$.

For this case, the twist in the field lines is localized around the spine and near the fan while being zero in the fan plane. In order to have a symmetric twist above and below the fan plane, even values of β must be chosen. As we wish to study a smooth transition from z independence to z dependence we choose to keep $\alpha \geq 4$ for $\beta \neq 0$ also. So we start with a field of the form

$$\mathbf{B} = B_0(r, jz^2 r^8 e^{-(r^2/l^2) - (c^2/l^2)(zr^2)^2}, -2z), \tag{19}$$

where we have chosen $\alpha=4$ and $\beta=2$ while including a non-zero c value to maintain localization.

Figure 3 shows the twist in the field that is again focused to a toroidal region around the spine with potential field surrounding it. However now the region has been pinched at the top and bottom by $c \neq 0$ and split to either side of the fan plane by the z power dependence ($\beta \neq 0$). Thus, on the fan itself the field lines are of potential form with the twist in the field existing in two tori on either side of it. The shape of these regions is clearly outlined by the shape of the current flow shown in the left panel of Fig. 4. We see that it is

oppositely directed above and below the fan plane and flows in a circuit within these squashed tori.

Figure 4, right and middle panels, shows the plasma flow which is also localized to these shaped regions with an extra counter rotating flow [marked out in red (solid) lines] that takes plasma in along the fan and out along the spine. This region is introduced by the extra damping due to $c \neq 0$ in the exponential term in Eq. (19). Another interesting aspect of this flow is that there is no outflow of plasma in the fan plane, even though because of the corotating nature of the plasma either side of this plane the plasma rotates around within it. This is a consequence of the z power dependence ($\beta \neq 0$).

We also find that because the perturbation is a multiple of r^2 all other higher even values of α give similar results. Note that for odd values of α , the z -component of the electric field has sinks and sources for $r \neq 0$, which is unphysical.

2. Opposite direction twist

To create a counter rotation of the field requires us to choose $\beta = \text{odd}$ in conjunction with $\alpha = \text{even}$. Since $\alpha \geq 4$ there are no constraints on the values β may take.

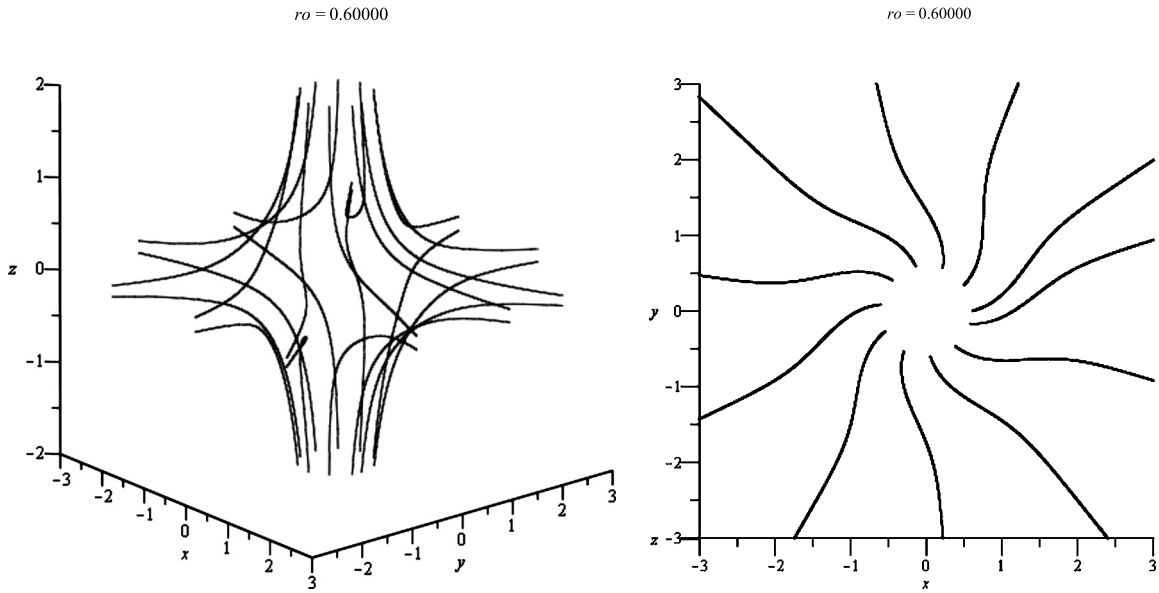


FIG. 3. Top and side views of field lines plotted for $\alpha=4$, $\beta=2$, and $c=0.2$ with $j=3$. The field lines close to the spine line are approaching the null and receding away from the null in the fan plane.

In this case we find that we have an oppositely directed twist in the field which is localized to two squashed tori, such that, once again, there is no twist in the fan plane. On either side of the fan plane the current density is equally directed but still of a similar general form as the previous z dependent symmetric case.

We also note that the flows above and below the fan are opposite to each other such that in the fan plane the plasma is static suggesting no flux is reconnected at the fan plane by this perturbation.

B. Torsional fan

We now consider a current term localized in height z . It is convenient to choose $\alpha=1$, $a=0$, and $b=1$ in Eq. (10) to yield field of the form

$$\mathbf{B} = B_0(r, jr(zr^2)^\beta z^\gamma e^{-(z^2/l^2)-(c^2/l^2)(zr^2)^2}, -2z), \tag{20}$$

where β and γ are positive integers. Using Eq. (7) the field line equations are

$$r = r_0 e^{B_0 s}, \quad z = z_0 e^{-2B_0 s}, \tag{21}$$

and

$$\phi = jB_0(z_0 r_0^2)^\beta e^{-(c^2/l^2)(z_0 r_0^2)^2} G(\gamma) + C, \tag{22}$$

where C is a constant of integration and $G(A)$ is defined as

$$G(A) = z_0^A \int e^{-2AB_0 s} e^{-(z_0^2/l^2)e^{-4B_0 s}} ds. \tag{23}$$

The recurrence relation for $G(A)$ is

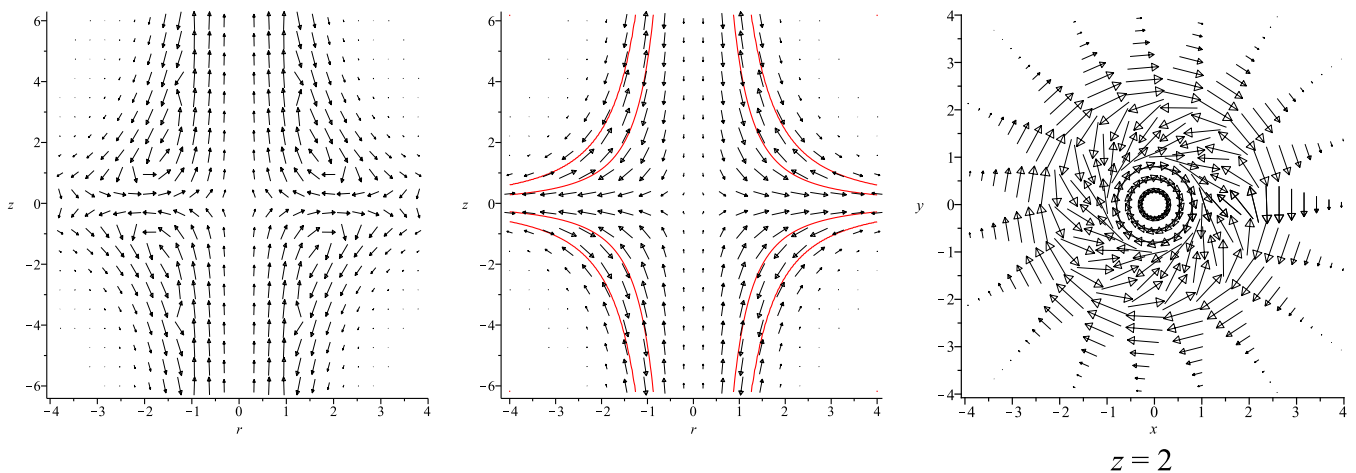


FIG. 4. (Color online) Scaled plots of the radially symmetric current flow (left panel) and plasma flows (middle and right panels) for $\alpha=4$, $\beta=2$, and $c=0.2$ with $l=1$ and $j=3$. Here, the maple scaling is applied with $d=13$ and r denotes either x or y .

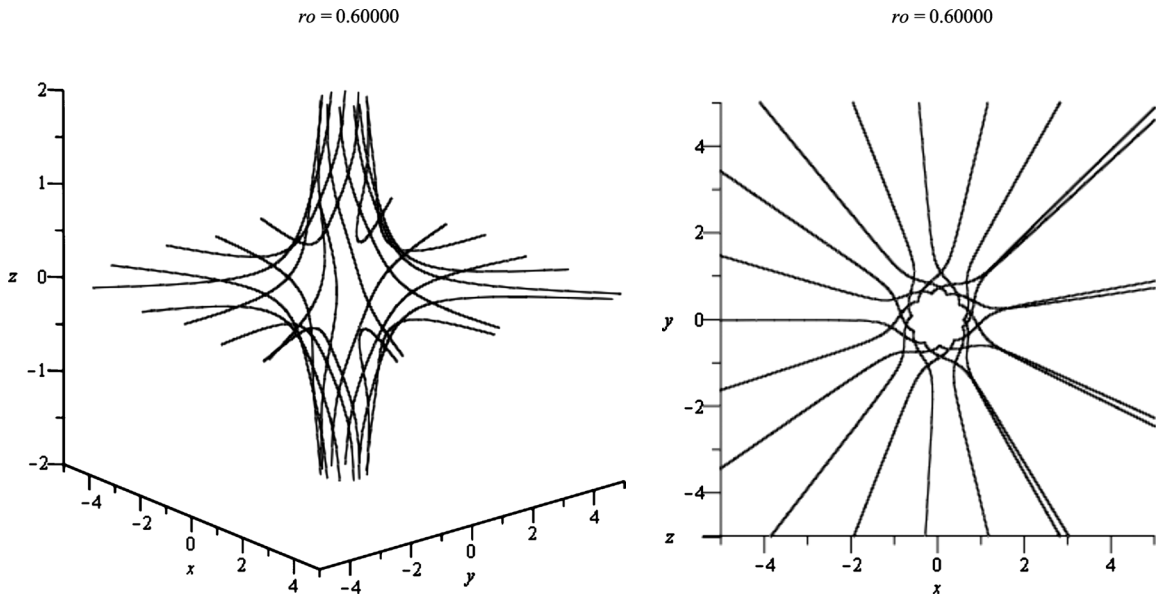


FIG. 5. Side and top view of field lines plotted for $\gamma=3$, $\beta=0$, $j=5$, $c=0$, and $l=1$. The field on the spine line is approaching the null and receding away from the null in the fan plane.

$$G(A+2) = \frac{l^2}{2} \left(AG(A) + \frac{z^A}{2B_0} e^{-z^2/l^2} \right), \quad (24)$$

where we can generate solutions for all values of A from

$$G(1) = -\frac{\sqrt{\pi}l}{4B_0} \operatorname{erf}\left(\frac{z}{l}\right), \quad (25)$$

$$G(2) = \frac{l^2}{4B_0} e^{-z^2/l^2}. \quad (26)$$

Using Eq. (4) we find the current

$$\mathbf{J} = \frac{jB_0}{\mu_0} \left(-\left((\gamma+\beta)z^{-1} - \frac{2}{l^2}(z+c^2(zr^2)^2z^{-1}) \right), 0, 2(1+\beta)r^{-1} - \frac{4c^2}{l^2}(zr^2)^2r^{-1} \right) r z^\gamma (zr^2)^\beta e^{-(z^2/l^2)-(c^2/l^2)(zr^2)^2} \quad (27)$$

and Eq. (6) gives us the electric potential as

$$\Phi = \frac{j\eta_0 B_0}{\mu_0} \left[z r^2 \left(\left((\gamma+\beta) - \frac{2c^2}{l^2}(zr^2)^2 \right) G(\gamma-2) - \frac{2}{l^2} G(\gamma) \right) + 2 \left(2(\beta+1) - \frac{4c^2}{l^2}(zr^2)^2 \right) G(\gamma+1) \right] (zr^2)^\beta e^{-(z^2/l^2)-(c^2/l^2)(zr^2)^2}. \quad (28)$$

It is clear that $\gamma \neq 0$ or 2 but there are no such constraints on β . In a similar manner to the previous section we now investigate further reconnection brought about by different choices of the various parameters.

1. Opposite direction twist

It is clear from Eq. (20) that to perturb the field in this way we need $\gamma+\beta$ to be odd, i.e., $\gamma=\text{odd}$ and $\beta=\text{even}$, or $\gamma=\text{even}$ and $\beta=\text{odd}$. A choice of the latter results in flows

containing sinks and sources similar to those in the torsional spine, $\alpha=\text{odd}$ case. We therefore only investigate in detail the $\gamma=\text{odd}$ and $\beta=\text{even}$ possibility.

a. The radially linear perturbation: $\beta=0$ and $c=0$.

In this case

$$\phi = jB_0 G(\gamma) + C. \quad (29)$$

The $\gamma=1$ case is a special case with a nonzero current that linearly increases with r in the fan plane which makes it different from the generic case of $\gamma \geq 3$. Thus we shall study the more generic case while pointing out any differences from the special case of $\gamma=1$. Let us consider $\gamma=3$ for which the field is given by

$$\mathbf{B} = B_0(r, jr z^3 e^{-z^2/l^2}, -2z). \quad (30)$$

Figure 5 shows how the twist in the field is localized to two flattened toroidal disklike regions above and below the fan plane. In Fig. 6 we see that the resulting current is localized to this region of twist and exists in two disks of opposite current within each of the twisted regions. Current disks of this kind were observed by Ref. 23.

Figure 6 (middle and right panels) shows the plasma flow. This flow counter rotates below the fan with static plasma in the fan plane separating the two regions. As a result of this, we have counter spiraling flows that move in along the fan and then spiral out close to the spine. Comparing to Fig. 2 we note that in the positive rz -plane the flows are in the opposite direction to torsional spine. As expected the flow is strongest in the two disklike twisted regions.

Note that the effect of increasing γ to higher odd values is to increase (decrease) the twist where $z > l$ ($z < l$) in an analogous way to the torsional spine case. Similarly increasing l also serves to reduce the damping of the exponential term with height and therefore to stretch the solution in z .

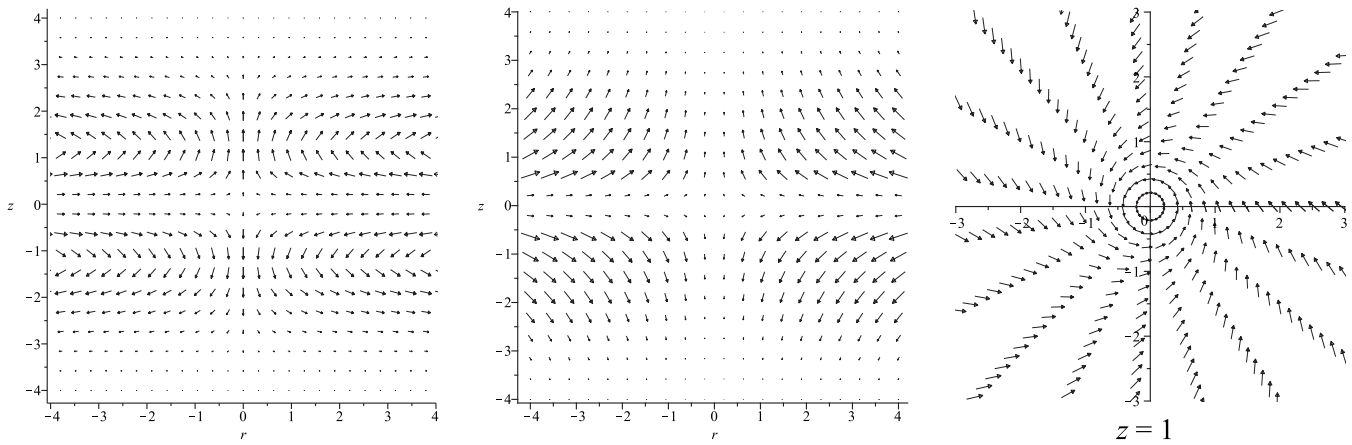


FIG. 6. Scaled plots of the radially symmetric current flow (left panel) and plasma flow (middle and right panels). Plotted for $\gamma=3$ and $\beta=0$ with $l=1$, $c=0$, and $j=5$. Here r denotes either x or y .

b. The radially nonlinear perturbation: $\beta \neq 0$ and $c \neq 0$.

Here we consider $\beta \neq 0$ and even. Since we are prohibited to choose $\gamma=0$ [see Eq. (28)] we consider the previous case of $\gamma=3$ combined with $\beta=2$ and a nonzero c value to maintain locality giving a field of the form

$$\mathbf{B} = B_0(r, jr^4z^5 e^{-(z^2/l^2)-(c^2/l^2)(zr^2)^2}, -2z). \tag{31}$$

The resulting field lines are shown in Fig. 7. The twist in the field lines is differentially varying with radius and localized to within two squashed tori on either side of the fan. Like the torsional spine case this is due to the extra damping, i.e., $c \neq 0$.

Figure 8, left panel, shows the resulting current that is localized to this region and rotates around within it. The middle and right panels of the figure show the plasma flow. The flows are much more complex than in the linear case. The original flow is sandwiched by counter rotating flows

from below and above. The flow in the vicinity of the fan plane results from the nonlinearity in r of the power law in the perturbation, i.e., through $\beta \neq 0$. This new flow spans both the spine and the fan becoming infinitely thin far away from the null, i.e., only the fan and the spine themselves. The second flow is a result of the nonlinearity in r of the exponential from $c \neq 0$. These flows are effectively the nonlinear radial nature of torsional spine reconnection asserting itself in the torsional fan regime.

Lastly, the $\gamma=1$ case behaves differently from the more generic cases of $\gamma \geq 3$. The smaller value of γ means that there is a linear plasma flow ($\beta=c=0$) down around the spine and out along the fan in the same manner as in the torsional spine reconnection. Therefore when the perturbation is made nonlinear in r the new flow is lost within the original one. We do however still see a counter rotating flow because of $c \neq 0$ but it is counter rotating in relation to the

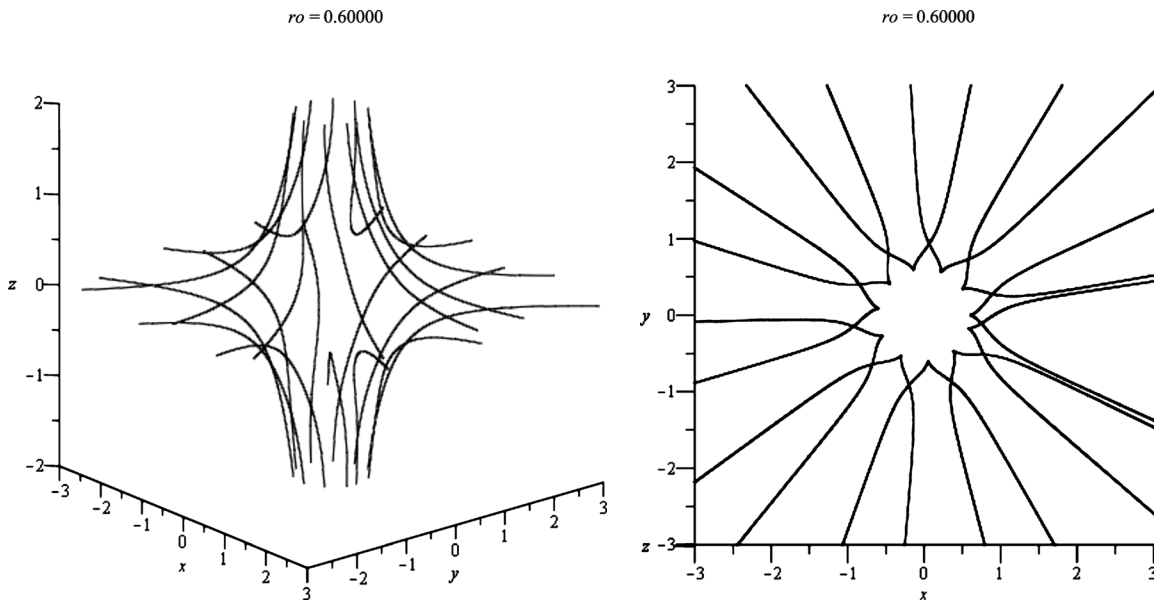


FIG. 7. Side and top views of field lines plotted for $\gamma=3$, $\beta=2$, $j=5$, $l=1$, and $c=0.2$. The field on the spine line is approaching the null and receding away from the null in the fan plane.

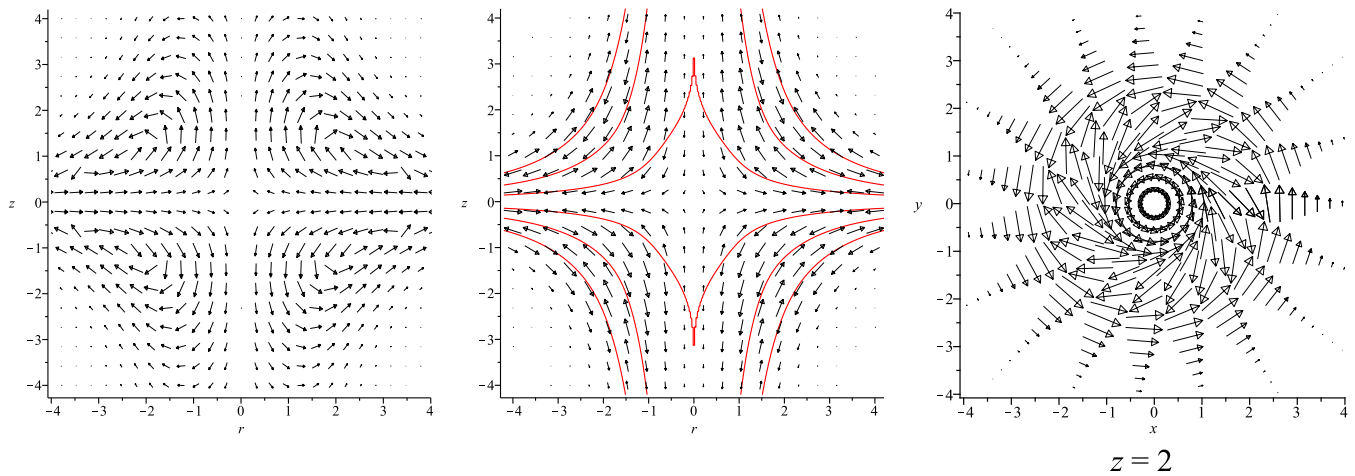


FIG. 8. (Color online) The left panel shows a slice of the scaled radially symmetric current flow, the middle and right panels showing the side and top views, respectively, of the scaled plasma flow when $\gamma=3$, $\beta=2$, and $c=0.2$ with $l=1$ and $j=5$ where $d=13$ with r denoting either x or y .

first flow and, therefore, is in the more generic direction for fan reconnection, along the fan and up the spine. Figure 9 illustrates this for the example of $\gamma=1$, $\beta=2$, and $c=0.2$.

So the overall picture of the plasma flow for the most generic, radially differentially varying counter twist, is a counter rotating spiraling flow, the majority of which travels along the fan and up around the spine with a portion of it counter rotating in relation to this first flow down the spine and out along the fan in two distinct regions. Static plasma in the fan separates the positive and negative z regions.

2. Same direction twist

As mentioned earlier the choice of γ =even is not a realistic solution to the problem so we consider γ and β both odd for this case. As an example, let

$$\mathbf{B} = B_0(r, jr^3z^4 e^{-(z^2/l^2)-(c^2/l^2)(zr^2)^2}, -2z), \tag{32}$$

where $\gamma=3$ and $\beta=1$ yield same direction twist field lines in the rz -plane. Such field lines result in a current density which is oppositely directed on either side of the fan plane while still being localized in a similar way to the previous current in Fig. 8. The plasma flows are again found to be counter rotating flows of the generic type described in the previous section except now the flow is equally directed on either side of the fan allowing for a rotating flow in the fan itself. Again for the $\gamma=1$ case the new flow is lost within that of the original due to its different directional nature.

IV. DISCUSSION

We have seen that for a twisting perturbation of the field around a 3D null current localizes to a torus within the per-

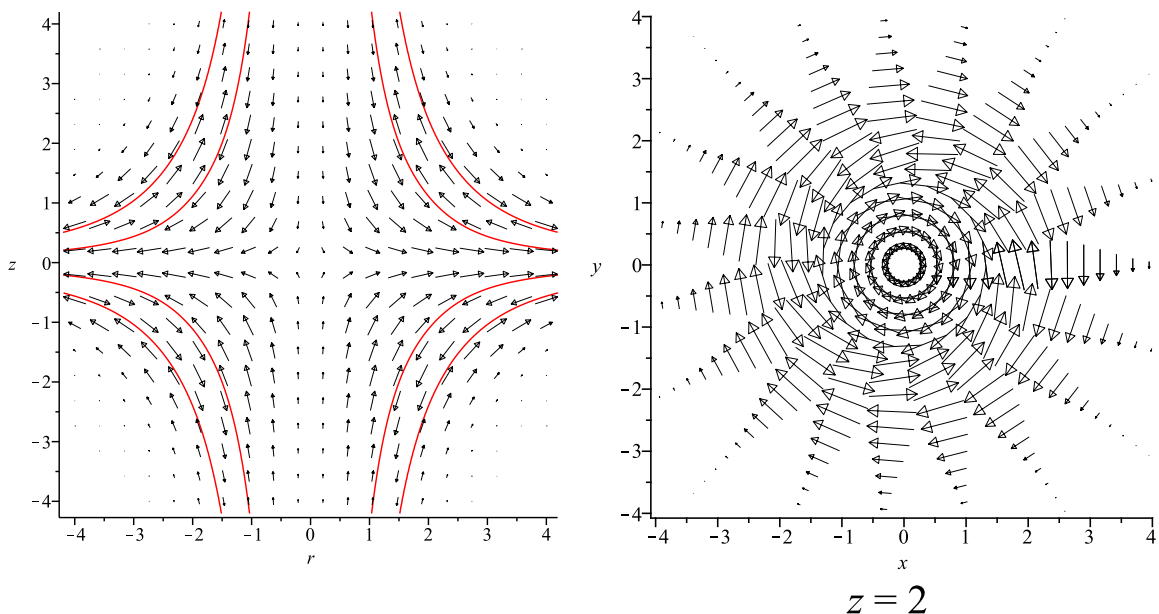


FIG. 9. (Color online) Top and side views of the scaled radially symmetric plasma flow for $\gamma=1$, $\beta=2$, and $a=0.2$ with $l=1$ and $j=5$, where $d=13$ with r denoting either x or y .

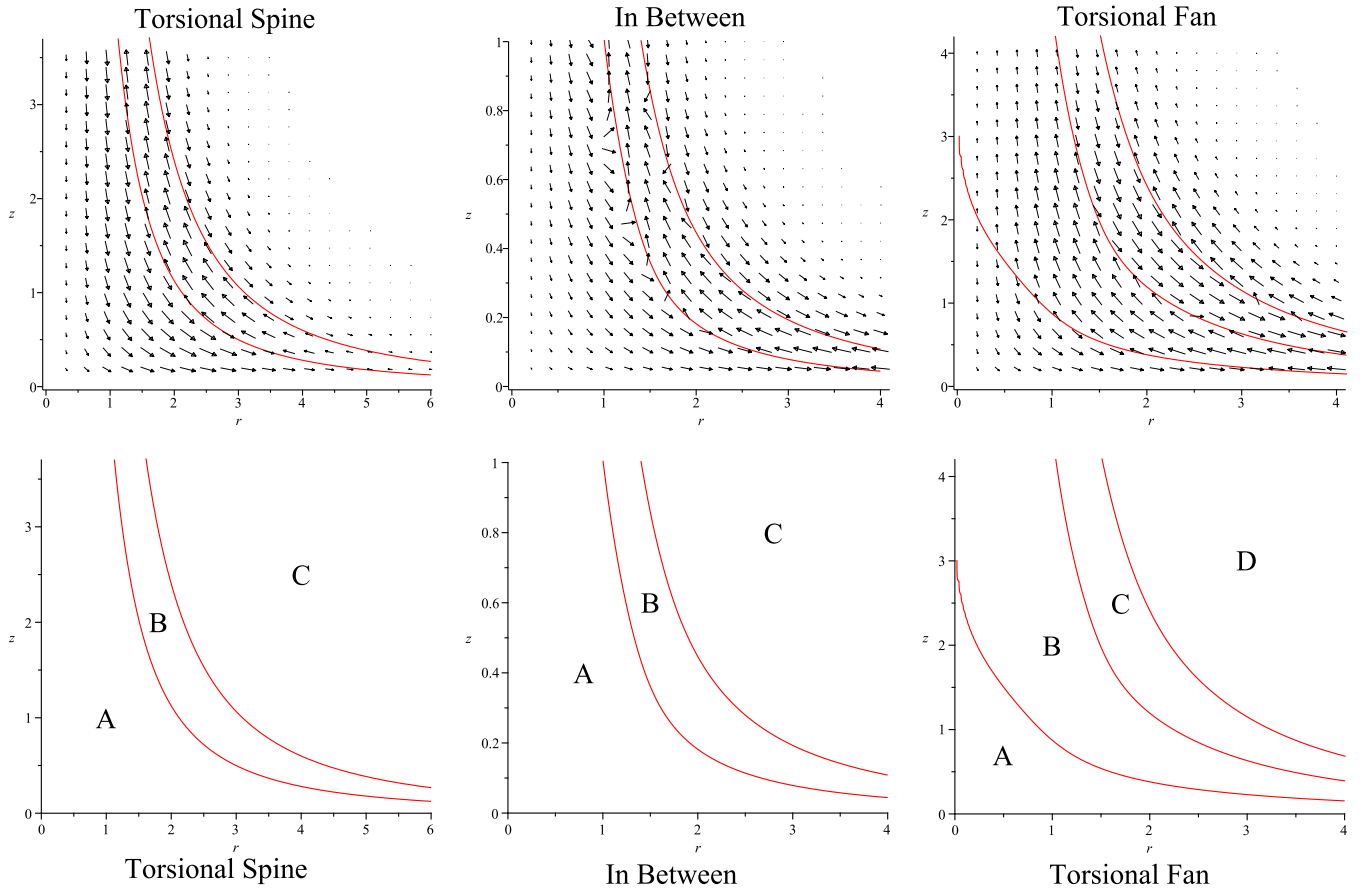


FIG. 10. (Color online) Flux transport regions in the positive rz -plane for the torsional spine ($\beta \neq 0$ and $c \neq 0$) and fan ($\beta \neq 0$, $\gamma \geq 3$, and $c \neq 0$) cases and the connecting regime between them. The top row shows the plasma direction while the bottom row separates regions in each regime. The solid red lines denote where $v_{\perp z} = 0$.

turbed region of field driving a slippage of the plasma through this region. Flux transport is therefore heavily dependent on the localization of the perturbation. The two main cases are that of localization around the spine or the fan. We have seen that the inclusion of terms with nonlinearity in r leads to torsional spine type flows and terms with nonlinearity in z lead to torsional fan type flows. Thus, we expect a smooth transition from one to the other. This requires an intermediate step: when $a=b=\gamma=\alpha=0$ with $c=\beta \neq 0$, resulting in a field of the form

$$\mathbf{B} = B_0(r, j(zr^2)^\beta e^{-(c^2/l^2)(zr^2)^2}, -2z). \quad (33)$$

A field of this form is perturbed in a way which has no bias to either spine or fan but varies differentially in zr^2 . In this case both electric potentials reduce to

$$\Phi = \frac{j\eta_0 B_0}{3\mu_0} \left\{ \left[\beta - \frac{2c^2}{l^2}(zr^2)^2 \right] \frac{r}{z} + 2 \left[2\beta + 1 - \frac{4c^2}{l^2}(zr^2)^2 \right] \frac{r}{z} \right\} (zr^2)^\beta e^{-(c^2/l^2)(zr^2)^2}. \quad (34)$$

Figure 10 shows how the two cases are linked by this term by focusing on the plasma flow in the positive rz -region since the direction of twist in this region remains the same for all values of α , γ , and β . The region **A** corresponds to pure z -independent torsional spine flow, **B** corresponds to

pure linear torsional fan flow, and **C** and **D** are associated with the damping from $c \neq 0$. We see how most of these flows appear in each case.

V. CONCLUSION

We investigated torsional magnetic reconnection at a 3D null point by allowing perturbations in the ϕ component of the magnetic field. We introduced models for the torsional spine and torsional fan reconnection regimes through solutions of the steady state kinematic resistive MHD equations. In both regimes we found spiral slippage of the field lines around the spine where we noted that this slippage is not involved in flux transport across the spine or the fan, i.e., flux is reconnected within the two topological distinct regions separated by the fan but not between them. This indicates that this kind of reconnection would not change the topological structure of an overall field but would act as an energy release for rotational stresses within it. We also found from the nature of the twist in the field that these stresses are manifest in currents focused around the spine for torsional spine and the fan for torsional fan agreeing with previous numerical studies.

We then investigated twists with nonlinearity in both r and z . The flows are found to be complex with competing effects between the two nonlinearities. We then linked the

two main cases with an intermediate step indicating that each of the “pure” linear regimes of torsional spine and fan are extreme cases of a general twist in the field.

ACKNOWLEDGMENTS

We thank D. Pontin and C. Parnell for many useful discussions. We also thank the anonymous referee for the thoughtful comments which helped improve this paper. P.W. is supported by EPSRC (U.K.) studentship.

- ¹I. J. D. Craig, R. B. Fabling, J. Heerikhuisen, and P. G. Watson, *Ap. J.* **523**, 838 (1999).
- ²K. Galsgaard and A. Nordlund, *J. Geophys. Res.* **102**, 231 (1997).
- ³Y. T. Lau and J. M. Finn, *Astrophys. J.* **350**, 672 (1990).
- ⁴D. W. Longcope, *Sol. Phys.* **169**, 91 (1996).
- ⁵D. W. Longcope and S. C. Cowley, *Phys. Plasmas* **3**, 2885 (1996).
- ⁶D. W. Longcope, *Phys. Plasmas* **8**, 5277 (2001).
- ⁷D. W. Longcope and I. Klapper, *Astrophys. J.* **579**, 468 (2002).
- ⁸D. I. Pontin and I. J. D. Craig, *Phys. Plasmas* **12**, 072112 (2005).
- ⁹E. R. Priest and V. S. Titov, *Philos. Trans. R. Soc. London, Ser. A* **354**, 2951 (1996).
- ¹⁰D. W. Longcope, D. S. Brown, and E. R. Priest, *Phys. Plasmas* **10**, 3321 (2003).
- ¹¹D. W. Longcope and C. E. Parnell, *Sol. Phys.* **254**, 51 (2009).
- ¹²S. Régnier, C. E. Parnell, and A. L. Haynes, *Astron. Astrophys.* **484**, L47 (2008).
- ¹³E. R. Priest, G. Hornig, and D. I. Pontin, *J. Geophys. Res.* **108**, 1285 (2003).
- ¹⁴E. Parlat, S. K. Antiochos, and C. R. De Vore, *Astrophys. J.* **691**, 61 (2009).
- ¹⁵T. Török, G. Aulanier, B. Schmieder, K. K. Reeves, and L. Golub, *Astrophys. J.* **704**, 485 (2009).
- ¹⁶M. L. Luoni, H. H. Mandrini, G. D. Cristiani, and P. Démoulin, *Adv. Space Res.* **39**, 1382 (2007).
- ¹⁷S. Masson, E. Parlat, G. Aulanier, and C. J. Schrijver, *Astrophys. J.* **700**, 559 (2009).
- ¹⁸I. Ugarte-Urra, H. P. Warren, and A. R. Winebarger, *Astrophys. J.* **662**, 1293 (2007).
- ¹⁹G. Barnes, *Astrophys. J. Lett.* **670**, L53 (2007).
- ²⁰C. J. Xioa, X. G. Wang, Z. Y. Pu, H. Zhao, J. X. Wang, Z. W. Ma, S. Y. Fu, M. G. Kivelson, Z. X. Liu, Q. G. Zong, G. H. Glassmeier, A. Balogh, A. Korth, H. Reme, and C. P. Escoubet, *Nature (London)* **2**, 478 (2006).
- ²¹D. I. Pontin, G. Hornig, and E. R. Priest, *Geophys. Astrophys. Fluid Dyn.* **98**, 407 (2004).
- ²²D. I. Pontin, G. Hornig, and E. R. Priest, *Geophys. Astrophys. Fluid Dyn.* **99**, 77 (2005).
- ²³D. I. Pontin and K. Galsgaard, *J. Geophys. Res.* **112**, 3103(2007).
- ²⁴K. Galsgaard, E. R. Priest, and V. S. Titov, *J. Geophys. Res.* **108**, 1042 (2003).
- ²⁵D. I. Pontin and E. R. Priest, *Phys. Plasmas* **16**, 122101 (2009).